Uncertainties of Urban Heat Island Estimation With Diverse Reference Delineation Methods Based on Urban–Rural Division and Local Climate Zone

Xuecheng Fu, Bao-Jie He, and Huimin Liu

***Abstract*—The precise quantification of surface urban heat island intensity (SUHII) is fundamental for understanding the process, causes, and solutions to thermal environmental change. However, the existing methods for SUHII estimation are not uniform in nonurban reference selection, with inconsistent consideration of relevant influencing factors. The associated uncertainty can be further exacerbated under seasonal fluctuations of atmospheric and surface environments. This study concentrated on macrocity and intraurban local scales to examine the variations in SUHII assessment and its seasonal changes using different reference delineation methods. City-scale analysis included eight references based on the fixed areas or dynamic buffers, while local-scale analysis took six natural cover types as references under the local climate zone (LCZ) framework, respectively. Results revealed significant differences in SUHII using diverse references, and the inconsistency varied across seasons. On the city scale, the most pronounced inter-method difference occurred in winter, while stronger consistency of spatial patterns was observed in summer. Relatively, higher seasonal SUHIIs and stronger spatial variabilities were generated by methods using fixed areas. On the local scale, a strong consistency of spatial patterns was also observed in summer, while the most pronounced difference occurred in spring. Maximum local SUHIIs in all seasons were obtained using LCZ G as a reference. The study further summarized a list of criteria of reference selection for both scales. Overall, this study provides empirical evidence supporting the appropriate reference delineation for reliable SUHII estimate, especially for seasonal analysis. It can facilitate an improved understanding of urban thermal variations and benefit effective urban heat mitigation.**

***Index Terms*—Local climate zone (LCZ), nonurban reference, seasonal variation, sensitivity test, surface urban heat island intensity (SUHII), urban–rural division.**

Received 12 July 2024; revised 26 August 2024 and 19 September 2024; accepted 30 September 2024. Date of publication 3 October 2024; date of current version 23 October 2024. This work was supported in part by the National Natural Science Foundation of China under Grant 42301339 and Grant 52308079, in part by the Fundamental Research Funds for the Central Universities under Grant 2024CDJXY014, in part by China Meteorological Administration Youth Innovation Team Project under Grant CMA2024QN15, in part by Chongqing Natural Science Foundation Project under Grant CSTB2024NSCQ-MSX0670, in part by the Natural Science Foundation of Hubei Province under Grant 2023AFB080, in part by the Key Laboratory of Earth Surface System and Human-Earth Relations under Grant LBXT2023YB04, and in part by the Tianjin Key Laboratory of Smart City Planning under Grant GHKF-202301. *(Corresponding author: Huimin Liu.)*

Xuecheng Fu is with the School of Architecture and Urban Planning, Chongqing University, Chongqing 400045, China, also with the Key Laboratory of New Technology for Construction of Cities in Mountain Area, Ministry of Education, Chongqing University, Chongqing 400045, China, and also with the Institute for Smart City of Chongqing University in Liyang, Chongqing University, Liyang 213300, China (e-mail: ferwinjohn@163.com).

Bao-Jie He is with the School of Architecture and Urban Planning, Chongqing University, Chongqing 400045, China, also with the Key Laboratory of New Technology for Construction of Cities in Mountain Area, Ministry of Education, Chongqing University, Chongqing 400045, China, also with the Institute for Smart City of Chongqing University in Liyang, Chongqing University, Liyang 213300, China, also with the School of Architecture, Design and Planning, The University of Queensland, Brisbane, QLD 4072, Australia, and also with the CMA Key Open Laboratory of Transforming Climate Resources to Economy, Chongqing 401147, China (e-mail: baojie.unsw@gmail.com).

Huimin Liu is with the School of Urban Design, Wuhan University, Wuhan 430072, China, also with the Research Center for Digital City, Wuhan University, Wuhan 430072, China, also with the Key Laboratory of Earth Surface System and Human-Earth Relations, Ministry of Natural Resources of China, Shenzhen 518055, China, and also with the Tianjin Key Laboratory of Smart City Planning, Tianjin 300110, China (e-mail: hmliu@whu.edu.cn).

Digital Object Identifier 10.1109/JSTARS.2024.3472475

I. Introduction

As THE spatial carriers of human economic, social, and cultural development, cities have experienced rapid development since the industrial revolution [1]. The region's original energy balance, hydrological cycle, and biogeochemical processes have been significantly disrupted by the accompanying high-intensity human activities and surface transformations. This has resulted in a series of ecological and environmental problems, including the deterioration of local climate, reduction of biodiversity, and environmental pollution [2]. Of particular note is the phenomenon of the urban heat island (UHI) effect, which is directly related to the health of urban dwellers and the habitability of the built environment [3]. As a consequence of urbanization, UHI is one of the most visible climatic changes and has been widely investigated and documented since the 20th century [4], [5]. In addition to exacerbating the existing public health concerns and introducing new risks, the intensification of UHI also indirectly contributes to adverse impacts, such as increased energy consumption and air pollution, which present a significant challenge to urban sustainability [6]. With further urban expansion/densification and the coupled effects of global warming, the adverse impacts described above will escalate, generating compound and cascading risks that are more complex and difficult to manage [7]. Consequently, the accurate assessment of UHI and the implementation of targeted mitigation-adaptation measures have received increasing attention and have become the focus of research in multidisciplinary fields.

Quantification studies of UHI can be divided into two categories according to the source of temperature data: atmospheric UHIs based on the air temperature data and surface urban heat islands (SUHI) based on the land surface temperatures (LSTs)

[8]. The former has commenced at an earlier stage, but data acquisition relies on a limited number of meteorological stations or instruments, which is limited in spatial representation continuity [9]. The latter has benefited from advances in remote sensing technology, and its advantages of wide spatial coverage, periodic observation, and data consistency can compensate for the shortcomings of the former in spatial information [10]. Therefore, this study focuses on SUHI. Extensive research has been conducted on the assessment of SUHI, and several indicators have been developed to quantify the characteristics of SUHI, including intensity, footprint, capacity, and so on [11]. Among the aforementioned indicators, the surface UHI intensity (SUHII) is one of the most widely used key indicators in current multiscale studies for its simplicity of calculation, comparability, and relative stability in response to climate fluctuations [12].

SUHII is measured in diverse ways at different scales. At the city scale, SUHII is typically defined as the LST difference between urban and nonurban reference area (an area not affected by urban development) under static conditions based on the urban–rural dichotomy or urban–rural gradient theory [13]. In fact, the heterogeneity of the urban thermal environment is not solely reflected in the macroscopic urban–rural contrast. Rather, it is also evident in the internal characteristics of the thermal environment within the urban area, which is not homogeneous due to its complex landscape composition, urban morphology, and human activities [14]. Furthermore, the high spatial overlap with human settlements makes it imperative to investigate local UHI within urban areas as a means to achieve refined knowledge benefit for the effective mitigation of microclimate change [15]. In local SUHII studies, thermal environment analysis is typically conducted in conjunction with urban zoning, encompassing a range of geographical units, including neighborhood patches, census units, local climate zones (LCZs), functional zones, and so on [16], [17], [18]. Among these, the LCZ offers a particularly effective means of integrating 2-D and 3-D information on regional patches, including land cover, building characteristics, morphology layout, and other relevant data. This approach has the potential to enhance the standardization of urban studies and facilitate a more nuanced and comprehensive understanding of urban microclimate characteristics [19]. LCZ has been widely used in the fields of climate assessment, urban planning, and sustainability, covering urban thermal health, building energy consumption, integration of multiscale climate models, urban development and governance strategies, and so on [20]. Current LCZ classification methods can be broadly categorized into GIS-based methods and image classification methods represented by the World Urban Database and Access Portal Tool (WUDAPT) [21]. Compared with the former, WUDAPT integrates professional knowledge and relies on remote sensing images, which has the advantages of lower data requirements, complete process, and relative simplicity, and has received general attention and application [22]. LCZ-based SUHI studies typically define local SUHII as the LST difference between built-type zones and land cover-type zones.

Nevertheless, current SUHII studies that focus on either its temporal dynamics or its spatial patterns are subject to uncertainty arising from their inconsistent methods for defining reference areas. There is no uniformity in the current literature regarding the selection of reference areas. For instance, at the urban scale, Siddiqui et al. [23] defined the nonurban area as a 5-km buffer outside the urban area boundary; Yao et al. [24] constructed a 10–30 km buffer around the urban area and excluded water bodies, impervious surfaces, and overheight pixels as the reference nonurban area; Li et al. [25] employed the modified equivalent area-rural method to define the reference area. Furthermore, the methods employed for defining local SUHII reference zones also differed from each other. For instance, Zhou et al. employed regional mean normalized LST as the reference temperature. In regard to the applications of the LCZ framework, diverse types, i.e., dense forest (LCZ A) [26], low vegetation (LCZ D) [27], and sparse trees (LCZ B) and water (LCZ G) as key components of urban green space [28], were, respectively, used as reference areas to quantify SUHII. These different reference delineation methods are often inconsistent in terms of both surface characteristics, such as land cover and landscape patterns, and human-made activities (infrastructure development, agricultural production activities, etc.). The associate conjoint impacts will diminish the accuracy of SUHII assessment and even lead to misinterpretation, creating difficulties for subsequent policy development and adaptation-mitigation measures.

Therefore, it is essential to investigate the sensitivity of SUHII assessment to different methods of reference delineation and further explore its variations across seasons. The sensitivity test to identify the optimal method at a specific scale is a fundamental step in guaranteeing the applicability and dependability of SUHII in evaluating the urban thermal environment and the suitability of subsequent policy measures. Furthermore, such sensitivity may also present pronounced seasonality, as seasonal fluctuations in thermal conditions and nonurban landscapes can directly alter its LST patterns, which complicates intermethod differences and amplifies the impact of associated uncertainty [29]. However, the existing limited number of studies exploring the uncertainty of SUHII assessment using difference references has rarely concerned its seasonal variations. This has resulted in an incomplete understanding of the seasonal dynamics of SUHI.

To fill the gaps mentioned above, this study conducted comparative experiments of seasonal SUHII estimates using different reference delineation methods at both city and local scales. The objective of this study is to do the following:

1) estimate SUHII on both city and interurban scales using diverse ways of reference delineation methods, respectively, based on urban–rural division and LCZ;
2) explore the spatial patterns and corresponding seasonal variations with different references;
3) summarize a sort of reference recommendation list for reliable SUHII estimate.

The results can benefit an improved understanding of SUHII and its seasonal variation patterns, and further facilitate effective urban heat mitigation.

II. Methodology

A. Study Area

The cities in the circum-Taihu Lake region (32.03°N–30.37°N, 119.14°E–121.34°E) were selected as the study cases

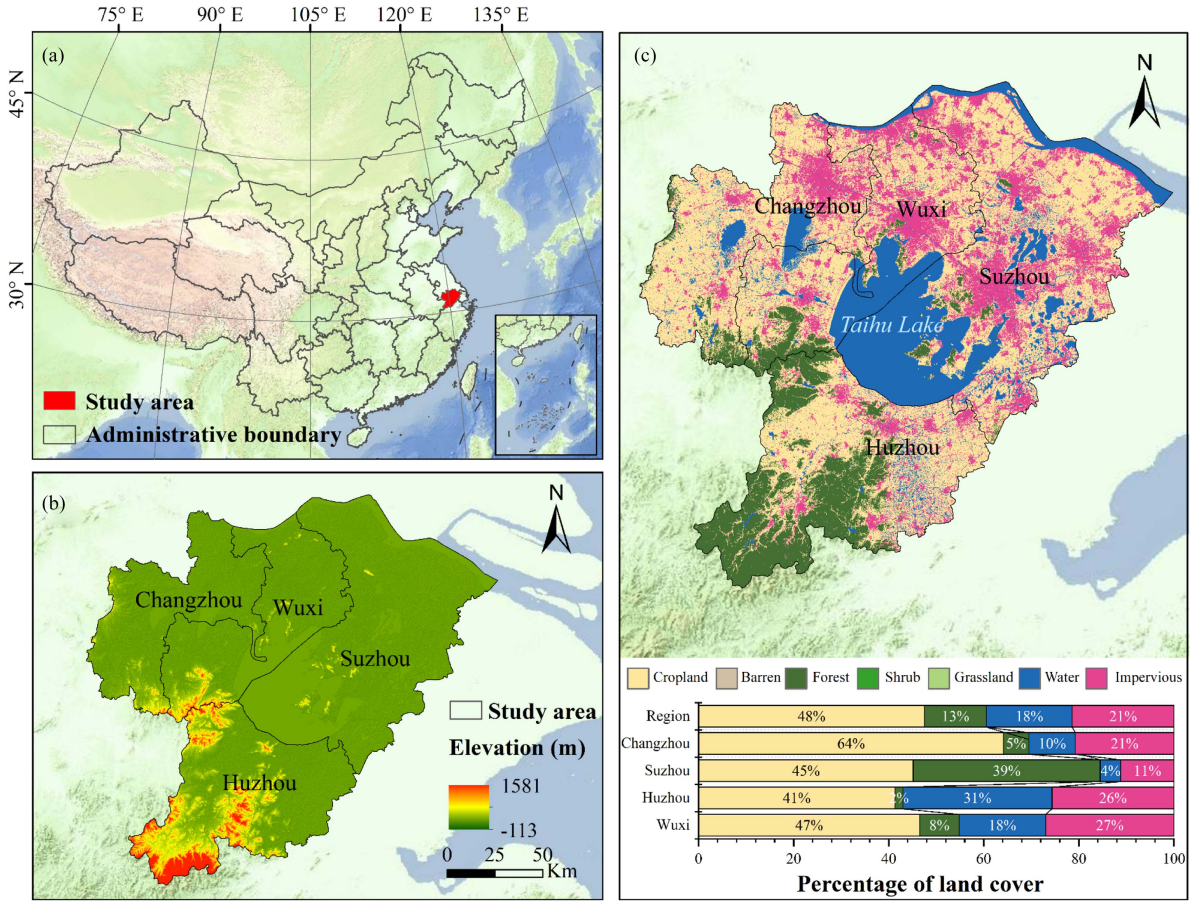

Fig. 1. Overview map of the circum-Taihu lake region. (a) Geographic location. (b) Regional elevation. (c) Regional land cover.

[see Fig. 1(a)]. The region is situated in the eastern part of China, with a total area of 23 489 km^2. It encompasses the four regional center cities of Changzhou, Wuxi, Suzhou, and Huzhou, as well as several satellite cities (Jintan, Liyang, Yixing, Anji, Deqing, etc.), which constitute an important part of the Yangtze River Delta region. The regional climate belongs to the subtropical monsoon climate, characterized by hot summers and warm winters, with simultaneous precipitation and high temperatures. The region's topography is predominantly plain, with elevated terrain in the southwest and low-lying areas in the northeast [see Fig. 1(b)]. The regional vegetation is characterized by subtropical evergreen broad-leaved forests. The region has experienced remarkable economic growth since the reform and opening up, with its GDP increasing from 371.943 billion yuan in 2000 to 5220.926 billion yuan in 2022, representing a 14-fold increase. The process of industrialization has led to the advancement of urbanization and a high degree of population agglomeration. By the end of 2022, the urban resident population within the administrative boundaries of Changzhou, Wuxi, Suzhou, and Huzhou has reached 4.2, 6.2, 10.6, and 2.2 million, respectively, and the population urbanization rates have reached 78.01%, 83.09%, 82.12%, and 66.4%, exceeding the national average (65.22%). Meanwhile, the amount of land required for urban development continues to increase, with the region's total impervious surface exceeding 21% by 2022 [see Fig. 1(c)]. However, the region is also confronted by prominent environmental issues and increased ecological vulnerability. In particular, urban sprawl and high-intensity construction has resulted in a deteriorated thermal environment and, consequently, exacerbated risks to the habitat environment [30].

B. LST Retrieval

Landsat 8-9 C2 L2 level data (processed with atmospheric corrections) from the U.S. Geological Survey[1] has been selected to obtain the 30-m LST through the single-channel algorithm. The Landsat series, which allows for the effective characterization of the surface thermal environment on a continuous spatial extent in a fine-grained way, has become the main source data for urban warming studies over the past half-century [31], [32]. In this study, four remote sensing images of 2022 were selected to reflect the seasonal variations of LST. The dates were 17 May [spring, Fig. 2(a)], 28 July [summer, Fig. 2(b)], 6 September [autumn, Fig. 2(c)], and 19 December [winter, Fig. 2(d)], respectively. The cloud cover of the aforementioned data was less than 10%. Furthermore, the data have undergone the requisite preprocessing, including radiometric correction, reprojection, cloud masking, quality control, unit conversion, and regional statistics.

[1][Online]. Available: https://earthexplorer.usgs.gov/

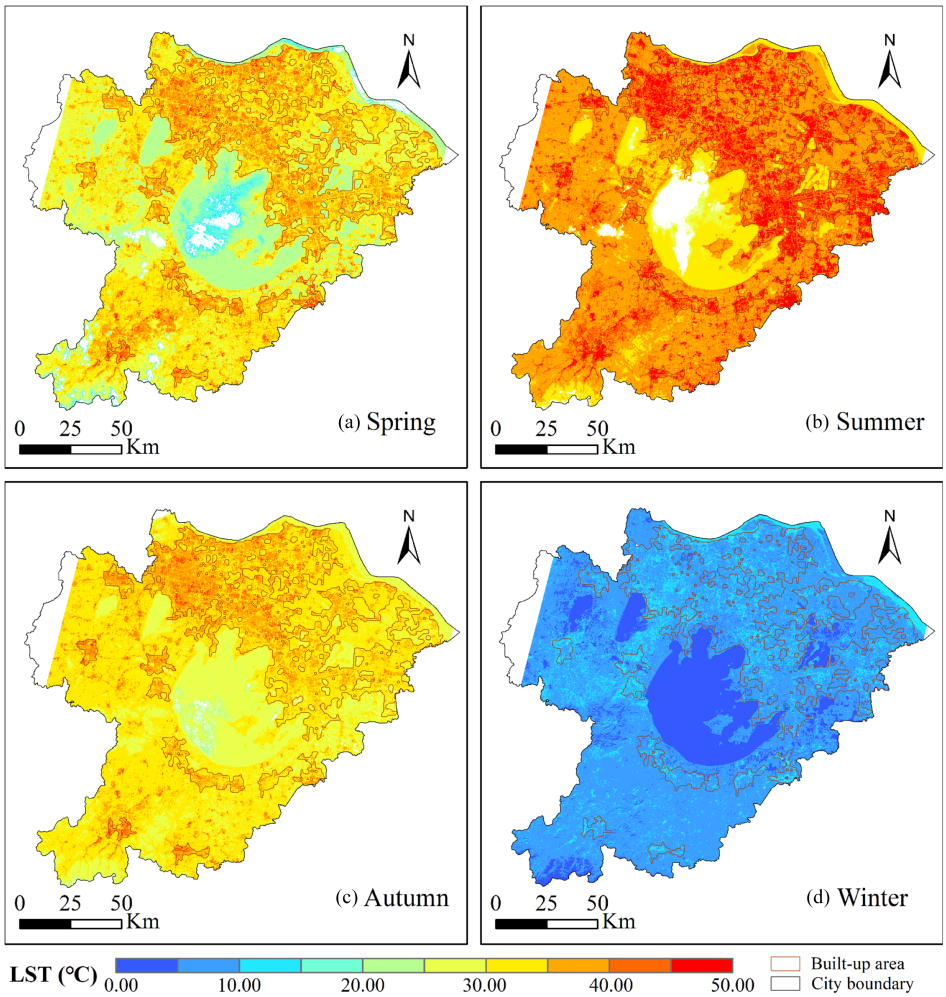

Fig. 2. Seasonal LSTs in the circum-Taihu region in 2022. (a) Spring. (b) Summer. (c) Autumn. (d) Winter.

C. City-Scale Nonurban Reference Delineation

The city-scale SUHII is defined by the LST difference (ΔT) between the urban area and the selected nonurban reference area. In detail, if ΔT is greater than 0 °C, it indicates the presence of a significant SUHI effect, whereas if ΔT is less than 0 °C, it indicates that the SUHI effect is not significant or even shows an urban cold island effect [10]. One of the principal contents of this study is the delineation of nonurban reference areas. Before this, the study employed a bottom-up city clustering algorithm to identify urban areas within the 2022 circum-Taihu Lake region. The following steps were employed:

1) to extract impervious surfaces in the study area based on the 30-m resolution China Land Cover Data;[2]
2) to construct a 1 km× 1 km grid to calculate and extract the grids with more than 50% of impervious surface, which can be considered as high development intensity units;
3) to aggregate the high development intensity units with a distance of 2 km.

Ultimately, a total of ten aggregated patches within the study area were identified as urban areas for the following analysis (see Fig. 3).

Based on this, eight categories of nonurban references were selected for the quantification of SUHII in this study (see Fig. 3). The method definitions and related references are presented in Table I. Among them, M1 and M2 were classified as fixed area reference delineation methods, while the remaining six methods were categorized as buffer area reference delineation methods based on the extent of the reference and the target urban area object. Furthermore, to avoid the influence of outliers, the study excludes internal water bodies (except for the stable landscape method), impervious surfaces, and overheight pixels (±50 m) within the nonurban reference areas based on the land cover data and the digital elevation model [45], [46].

D. Local-Scale Nonurban Reference Delineation

This study presented a comparative analysis of local SUHII obtained by nonurban reference delineation methods based on LCZs. It used the WUDAPT system to map the LCZ of the circum-Taihu region in 2022 and to further conduct

[2][Online]. Available: https://zenodo.org/records/8176941

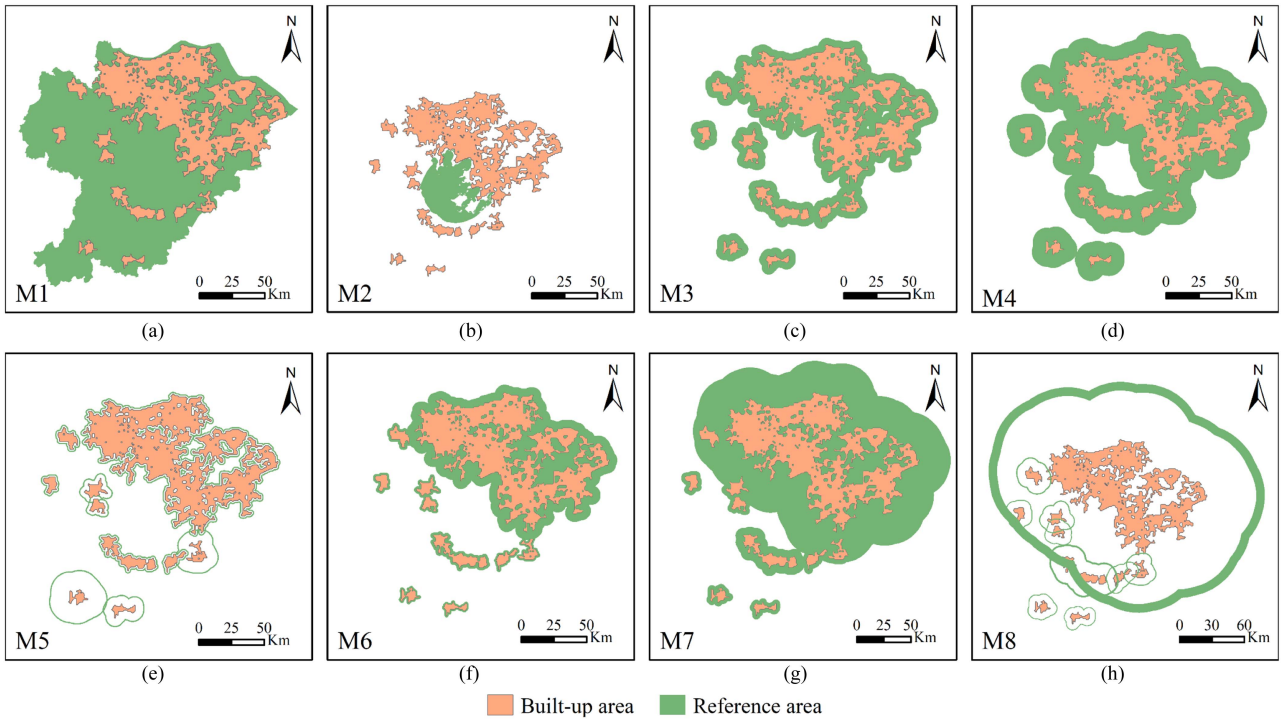

Fig. 3. Nonurban areas defined by the eight nonurban area reference delineation methods (in summer). (a) Administrative division method. (b) Stable landscape method. (c) 5-km fixed buffer method. (d) 10-km fixed buffer method. (e) Turning point method. (f) Equal area method. (g) Equal radius method. (h) Footprint-based method.

TABLE I
URBAN-SCALE NONURBAN REFERENCE DELINEATION METHODS

Code	Method name	Definition of non-urban reference area	Reference
M1	Administrative division method	The remaining administrative divisions except for the identified urban areas.	[12], [33]
M2	Stable landscape method	The landscape with stable distribution and attributes. In this study, Lake Taihu was selected as the reference area.	[33], [34]
M3	5-km fixed buffer method	The surrounding area within a buffer distance of 5 km outside the city boundary.	[35], [36]
M4	10-km fixed buffer method	The surrounding area within a buffer distance of 10 km outside the city boundary.	[37, 38]
M5	Turning point method	The buffer presenting the first turning point of LST, which was visually identified based on continuous 1 km buffers.	[39], [40]
M6	Equal area method	The buffer of an identical size to the urban area outside the urban boundary.	[15], [41]
M7	Equal radius method	The buffer outside the urban boundary, with a radius equal to that of a circle of the same area as the urban area.	[40], [42]
M8	Footprint-based method	Taking into account the urban size and SUHI footprint, multi-ring equal area buffers were generated and the sixth buffer was selected.	[43], [44]

local-scale SUHII comparisons using references delineated with different LCZ types. WUDAPT was developed by Ching et al. [47] with supervised classification of Landsat images based on urban morphology using the random forest classification algorithm. The algorithm employed a classification system based on the reflected radiation patterns of multispectral bands in selected multitype training regions [48]. The WUDAPT LCZ standard classification process consists of four steps.

1) Select typical LCZ areas to be used as training samples based on the WUDAPT project guidelines, prior knowledge, and other auxiliary data (e.g., land cover, building layout, building height, etc.).
2) Based on the WUDAPT process framework, the 2022 Landsat remote sensing images were preprocessed by reprojection, resampling (from 30 to 100 m), clipping and imported into SAGA GIS software.
3) Supervised classification of the target area using the LCZ classification tool (random forest based classifier) in the software and applying filtering to obtain a more homogeneous map.
4) Accuracy assessment of the output results.

Fig. 4 presents the final LCZ map of the study area in 2022. The overall classification accuracy of the urban area, as determined by random sampling verification of Google Earth images, was 77.82%, which met the accuracy requirements.

TABLE II
LST STATISTICS FOR URBAN AREAS AND REFERENCE AREAS IN THE STUDY AREA, 2022

Statistical subdivision		Urban area	M1	M2	M3	M4	M5	M6	M7	M8
Spring	Avg	36.18	31.01	23.47	31.58	31.50	30.05	31.65	31.48	31.52
	Std	1.38	3.42	2.10	2.94	3.05	3.48	2.89	2.91	2.99
Summer	Avg	43.71	38.42	33.90	38.59	38.72	37.88	38.69	38.83	38.72
	Std	2.30	2.42	1.74	2.32	2.45	2.31	2.32	2.37	2.31
Autumn	Avg	36.06	32.15	29.30	32.45	32.36	31.45	32.63	32.60	32.22
	Std	1.63	1.99	1.03	1.66	1.72	1.76	1.69	1.65	1.71
Winter	Avg	9.30	8.10	4.49	8.40	8.28	7.94	8.61	8.45	8.10
	Std	0.53	1.78	0.99	1.59	1.68	1.99	1.48	1.55	1.73

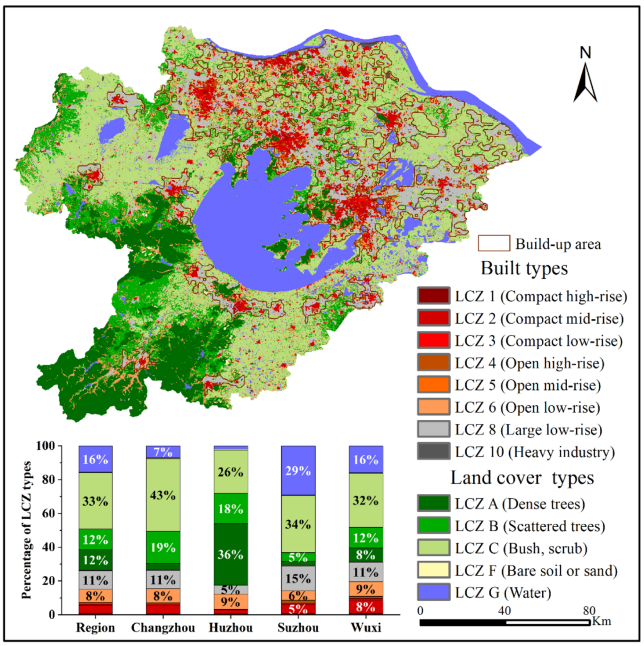

Fig. 4. Distribution and statistics of the LCZs in the circum-Taihu lake in 2022.

The LCZ-based local SUHII is usually defined as the LST difference between the built-type zone and the land cover zone. In this study, due to the limited samples of LCZ D (low plants) and LCZ E (Bare rock or paved) in the region, it was necessary to reclassify LCZ D as its similar type of LCZ C (bush and scrub) and LCZ E as a neighboring building-type LCZ in the classification process. On this basis, the study selected the overall land cover zone (LCZ N) and each type of land cover zone (LCZ A, LCZ B, LCZ C, LCZ F, and LCZ G) as the nonurban references for calculating SUHII for overall and each type of built-type zone (LCZ 1, LCZ 2, LCZ 3, LCZ 4, LCZ 5, LCZ 6, LCZ 8, and LCZ 10), respectively.

III. RESULT

A. Impact of Different Reference Delineation Methods on Urban-Scale Seasonal SUHII Assessment

The study summarized the LST levels in the urban areas and multiple nonurban reference areas in 2022 (see Table II). First, the region presented the SUHI effect (ΔT>0 °C) with the LSTs in nonurban areas, whichever reference delineation method was used, being lower than those in built-up urban areas. A comparison among all eight methods revealed that the M6 generated the highest reference LSTs in spring (31.65 °C), autumn (32.63 °C), and winter (8.61 °C). By contrast, in summer, the highest reference LST was obtained by M7, reaching 38.83 °C. Furthermore, the reference areas delineated by M2 exhibited lower LST values throughout the year. Notably, it was observed that, except for M2, all other methods generated reference LSTs with the standard deviations being higher than that of the urban areas, indicating greater LST variability in these reference areas.

The seasonal variations of the SUHIIs estimated using different references were presented in box plots (see Fig. 5). On average, covering SUHIIs estimated using all reference delineation methods, the interseasonal SUHII variations exhibited a pattern with spring (5.90 °C) > summer (5.74 °C) > autumn (4.17 °C) > winter (1.51 °C). Furthermore, the study was subjected to analysis using ANOVA and post hoc multiple comparisons REGWQ methods, which revealed that SUHII values obtained from different reference delineation methods within each season exhibited considerable variability (see Fig. 5). The greatest variability in SUHII was observed in winter ($F = 117.43$ and $p<0.01$), followed by spring ($F = 75.92$ and $p<0.01$), summer ($F = 10.79$ and $p<0.01$), and autumn ($F = 8.62$ and $p<0.01$). A comparison among all methods revealed that the highest SUHII was obtained using M2, with 12.72 °C in spring, 9.82 °C in summer, 6.77 °C in autumn, and 4.82 °C in winter. In comparison, the lowest SUHII in spring (4.53 °C), autumn (3.43 °C), and winter (0.70 °C) was obtained using M6, while the lowest value in summer (4.89 °C) was obtained by M7. Besides, there was a significant difference among seasons while using the same reference delineation method ($p<0.01$). The interseasonal variability among eight methods was quantified as M6 ($F = 78.57$) > M3 ($F = 59.67$) > M4 ($F = 52.43$) > M7 ($F = 46.37$) > M2 ($F = 44.41$) > M5 ($F = 31.27$) > M8 ($F = 27.64$) > M1 ($F = 13.32$).

Furthermore, the spatial patterns of SUHIIs estimated by specific area reference delineation methods (M1 and M2) exhibited greater standard deviations, namely, greater spatial variability, in comparison with the other six buffer area methods (see Fig. 6). The study further examined the spatial pattern consistency of SUHII results obtained using different reference delineation

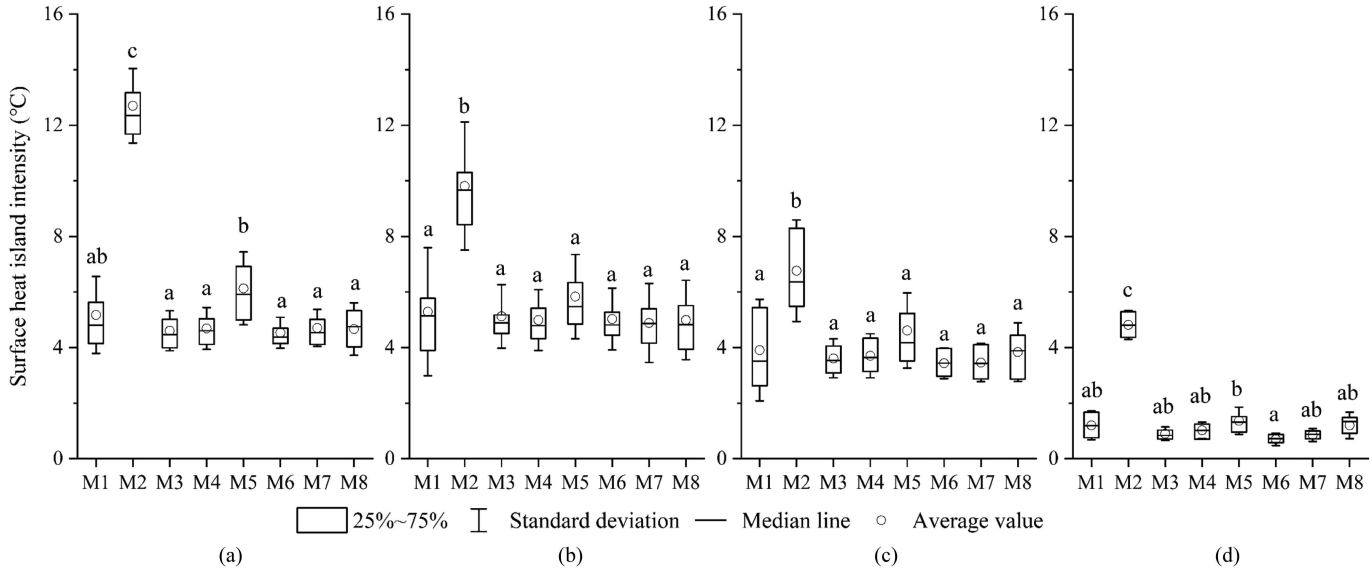

Fig. 5. Box plots of city-scale seasonal SUHII estimated based on the different reference delineation methods. Note: Different letters represent significant differences between methods, e.g., *a* and *b*, while *ab* indicates a nonsignificant difference between them. (a) Spring. (b) Summer. (c) Autumn. (d) Winter.

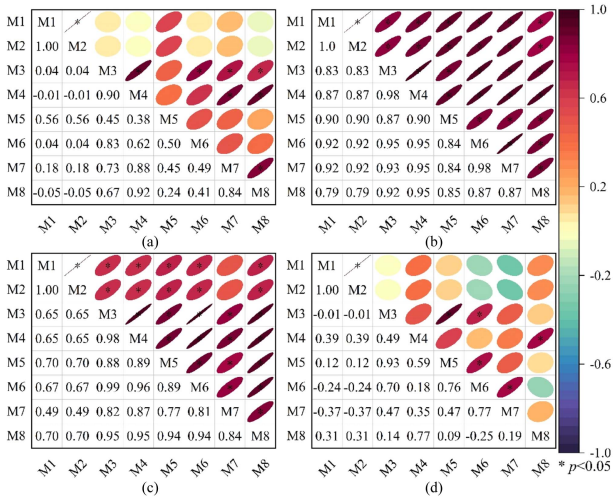

Fig. 6. Correlation coefficients of city-scale SUHIIs between any pair of reference delineation methods for all seasons. Note: Larger ellipse area indicated a greater standard deviation of data distribution; larger values represent a greater consistency in the distribution of the data. (a) Spring. (b) Summer. (c) Autumn. (d) Winter.

methods in combination with Spearman correlation analysis. Overall, the strongest correlations were observed in summer and autumn, which were significantly larger than those in spring and winter. This indicates that, at the city scale, the spatial distributions of SUHII obtained by different methods exhibited higher degrees of consistency in summer and autumn, while exhibiting weaker or even opposing distribution characteristics in spring and winter. In detail, in spring, the SUHII estimated by all eight methods showed positive correlations, especially between the SUHII obtained by the buffer area reference delineation methods. There were significant relationships between M3-M4-M7-M8 and between M3-M6 ($p<0.05$). In contrast, the correlation between the results generated by the fixed area reference methods (M1 and M2) and the other methods was low and not even significant; in summer and autumn, the SUHII estimated by each method exhibited high positive correlations, with the relationships being significant in all cases except between M1 and M7 in autumn. In comparison with the other seasons, the correlation coefficients between methods were generally lower in winter, with the relationships being significant only between M3-M5-M6, M6-M7, and M4-M8.

B. Impact of Different Reference Delineation Methods on Local-Scale Seasonal SUHII Assessment

The study obtained the LCZ mapping of the circum-Taihu region based on the WUDAPT system process and conducted a statistical analysis regarding the LSTs in each zone across all seasons (see Table III). The results demonstrated that among the built-type LCZs, the higher values of spring and summer LST were observed in the LCZ 3 region, reaching 39.09 °C and 46.92 °C, respectively. In contrast, in autumn and winter, they were observed in the LCZ 8 region, reaching 38.18 °C and 10.26 °C, respectively. Overall, the lowest LST values were observed in LCZ 10 (spring, 34.31 °C), LCZ 6 (summer, 42.08 °C), and LCZ 4 (autumn, 34.90 °C; winter, 7.91 °C). Furthermore, in all seasons, the LSTs were generally lower for the land cover types of LCZ than for the built types. Among the land cover types, the higher LSTs were observed in LCZ F during the spring, summer, and autumn months, reaching 33.54 °C, 41.89 °C, and 34.44 °C, respectively. In contrast, during the winter, higher LST was observed in LCZ B (9.10 °C). The lowest values of seasonal LST for the land cover types were all distributed in LCZ G. Furthermore, it was found that the land cover types exhibited greater variability among LCZs compared with the built-type LCZs. Specifically, LCZ 5 and LCZ 10 in the built types and LCZ F in the land cover type showed greater variability within their respective LCZ category.

TABLE III
SEASONAL LST STATISTICS FOR BUILT-TYPE AND LAND COVER-TYPE LCZ, 2022

LCZ Type	Category	Built								Land cover				
		LCZ 1	LCZ 2	LCZ 3	LCZ 4	LCZ 5	LCZ 6	LCZ 8	LCZ 10	LCZ A	LCZ B	LCZ C	LCZ F	LCZ G
Spring	Avg	36.60	37.67	39.09	34.66	35.59	34.75	38.91	34.31	29.95	32.67	33.17	33.54	27.14
	Std	1.55	1.72	1.57	1.19	2.79	1.44	1.69	3.35	1.97	1.57	1.23	3.53	2.19
Summer	Avg	44.13	45.50	46.92	42.82	43.60	42.08	46.64	42.77	38.40	39.75	39.86	41.89	36.94
	Std	2.01	2.43	2.79	1.74	3.19	1.49	2.77	3.30	1.19	1.45	1.22	2.35	1.61
Autumn	Avg	36.03	36.91	37.83	34.90	35.47	35.07	38.18	35.16	32.23	33.75	33.59	34.44	30.79
	Std	2.08	2.27	2.61	1.60	2.68	1.70	2.01	2.39	1.00	1.54	1.60	2.43	1.56
Winter	Avg	8.37	8.68	9.24	7.91	8.75	9.06	10.26	9.75	8.36	9.10	8.86	8.21	7.04
	Std	0.83	0.55	0.64	0.75	0.92	0.56	0.73	1.07	1.12	0.58	0.73	1.41	1.30

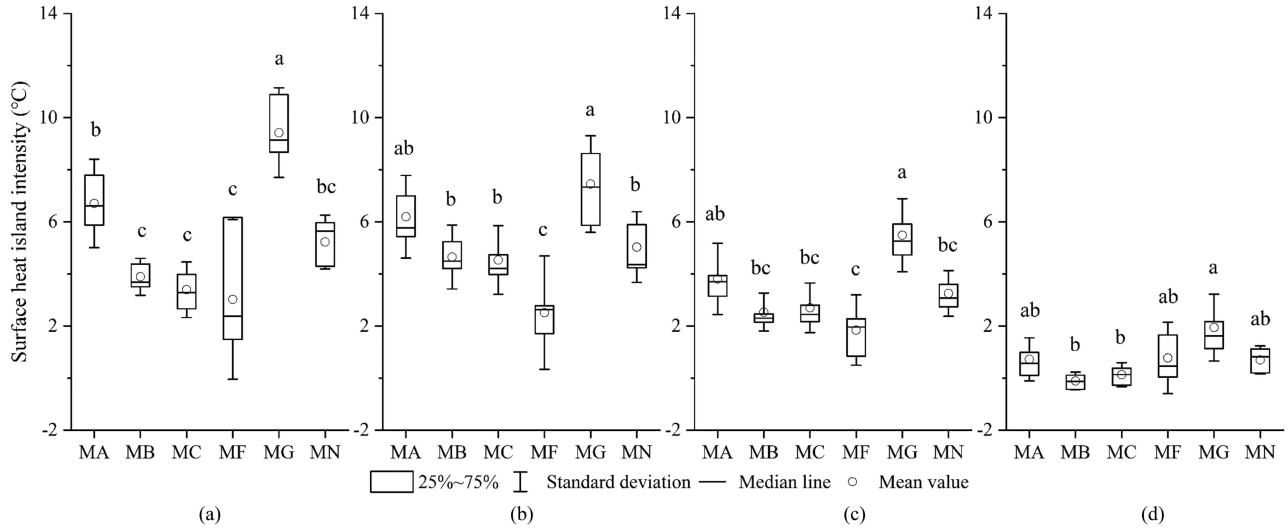

Fig. 7. Box plots of local-scale seasonal SUHII estimated based on different LCZ references. (a) Spring. (b) Summer. (c) Autumn. (d) Winter.

In this study, the land cover-type LCZs were selected as references to local-scale SUHII (see Fig. 7). In general, SUHIIs estimated using all reference delineation methods exhibited a pattern with spring (5.26 °C) > summer (5.04 °C) > autumn (3.26 °C) > winter (0.69 °C). Meanwhile, the local-scale SUHII estimates demonstrated considerable intermethod variability, which was most pronounced in spring (F = 19.73), followed by autumn (F = 12.43), summer (F = 10.50), and winter (F = 6.28). The local SUHII values estimated based on the MG (water) method were found to be significantly higher than those of the other methods in all seasons, reaching 9.43 °C (spring), 7.45 °C (summer), 5.49 °C (autumn) and 1.94 °C (winter), respectively. In contrast, the local SUHII obtained by the MF (bare soil or sand) and MB (scattered trees) methods is lower, especially the winter local SUHIIs obtained by MB, which was less than 0 °C, i.e., it showed a cold island effect opposite to the results obtained by other methods. In addition, the study found significant seasonal variability in the results obtained by each reference method. Specifically, the interseasonal variability of the methods was categorized in descending order as MB (F = 66.14) > MN (F = 44.59) > MG (F = 40.63) > MC (F = 34.72) > MA (F = 33.84) > MF (F = 2.11).

About the spatial distribution patterns of local SUHIIs (see Fig. 8), it was observed that, among all six methods, the standard

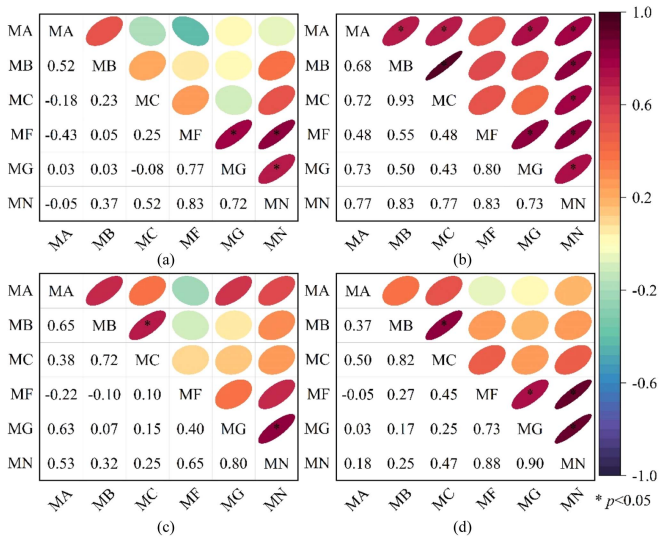

Fig. 8. Correlation coefficients of local-scale SUHIIs between any pair of reference delineation methods for all seasons. Note: Larger ellipse area indicated the greater standard deviation of data distribution; larger values represent the greater consistency in the distribution of the data. (a) Spring. (b) Summer. (c) Autumn. (d) Winter.

deviation of SUHII obtained using MF was greater in spring, summer, and winter, while MG yielded higher values in autumn. In contrast, SUHII estimated by MB showed less spatial variation in all seasons. In terms of the spatial pattern consistency under different reference delineation methods, it is found that the results exhibited strong spatial consistency in summer, which was greater than that in winter, autumn, and spring, sequentially. In detail, in the spring, the majority of the results obtained by the methods showed lower and even negative correlations. Only the results obtained by MG-MF-MN were significantly correlated in a positive manner ($p<0.05$). In contrast, summer showed a general positive correlation between the methods, and more than half of the pairwise relationships were significant. In autumn and winter, the relationships between SUHII results exhibited similar characteristics to those observed in the spring, namely low correlations and a limited number of significant correlations. Only the relationships between MB-MC (autumn and winter), MG-MN (autumn and winter), MF-MG (winter), and MF-MN (winter) were found to be significant.

Beyond the analyses that considered the built-type LCZs as a whole, the study further explored the impact of reference delineation on the assessment of SUHII to its subcategories (see Fig. 9). Overall, seasonal SUHII obtained by different methods showed a general and significant variability ($p<0.01$) across LCZs of each built type. The greatest variability in SUHII obtained by different methods occurred in spring for LCZ 1, LCZ 2, LCZ 3, LCZ 5, LCZ 8, and LCZ 10, in autumn for LCZ 4, and in summer for LCZ 6. In winter, SUHII variability was generally low across the LCZs. The local significant high SUHIIs obtained based on MG were also validated in each built-type LCZ compared with other reference methods. Overall, the higher values of SUHII in spring (11.96 °C) and summer (9.98 °C) occurred in LCZ 3, and higher values in autumn (7.39 °C) and winter (3.22 °C) occurred in LCZ 8. Furthermore, the greatest interseasonal variations in SUHII were obtained based on MG and MA, with the former commonly occurring in LCZ 1, LCZ 2, LCZ 3, LCZ 4, LCZ 5, LCZ 6, LCZ 8, and the latter in LCZ 10.

Spatially, a more discrete distribution pattern of local SUHIIs obtained by MF was observed for most of the built-type LCZs. The study examined the consistency of SUHII results across different reference delineation methods for each built-type LCZ, in conjunction with correlation analyses (see Figs. 10 and 11). The results demonstrated that the spatial consistency of SUHII results varied among built-type LCZs and exhibited evident seasonal instability. In general, the high levels of correlations were mainly observed in summer (LCZ 1, LCZ 2, LCZ 3, LCZ 4, and LCZ 5) and autumn (LCZ 6, LCZ 8, and LCZ 10). This indicated that, for the aforementioned LCZs, the SUHII results quantified by each method exhibited a high degree of consistency in the corresponding seasons. In contrast, during spring (LCZ 1, LCZ 2, LCZ 3, LCZ 5, LCZ 8, and LCZ 10), autumn (LCZ 4), and winter (LCZ 6) seasons, the SUHII pairwise relationship correlations were low or even exhibited negative correlations. This suggested that the spatial distribution patterns of SUHII were unstable or even opposite among the different methods.

IV. Discussion

A. Uncertainty Introduced by Reference Selection for SUHII Quantification

The quantification of SUHII at the urban scale is subject to multiple uncertainties that may affect the accuracy and reliability of the research results. These uncertainties include differences in geographical condition (topography and climate), methodology (measurement methods and data sources), study scale (time and space), reference areas area selection, and type and intensity of human activities, among others [49]. In particular, the uncertainty associated with reference selection arises whenever the definition of the SUHI is misunderstood as the simple temperature difference between urban and nonurban reference areas and the references are not selected to highlight the impact of urban effects [33]. This is, therefore, a primary and fundamental problem in reliable urban climate research. Reference areas, which serve as the spatial carriers of many climate-associated features (land cover, meteorological conditions, topographic relief, etc.), present varying temperature levels across time and space [50]. Therefore, the selection of appropriate reference areas is of paramount importance for the accurate calculation of SUHII, especially for comparative studies across time or space.

The study compared and analyzed the SUHII obtained by the existing mainstream reference delineation methods, and the results revealed significant horizontal intermethod and vertical interseasonal differences. First, the discrepancy in SUHII estimates obtained by different methods is due to the inconsistency in the extent of nonurban areas and their internal surface characteristics obtained by different methods. This is evidenced by the disparate fixed-specific areas (M1 and M2) and buffer distances (M3, M4, M5, M6, M7, and M8). Specifically, the former provides a consistent reference point. With a fixed region selected, data collection and analysis are relatively simple, facilitating repeated experiments and comparative studies across cities. However, the fixed-area reference faces the impact of uncertainty brought about by differences in factors, such as regional environment, land cover, size, and location For instance, as for the two fixed-area reference methods, the area delineated by the administrative division method encompasses a diverse array of land covers (woodland, grassland, water bodies, cropland, etc.) and local topographic variations, whereas the area of the stable landscape method is constituted solely of water bodies and is relatively smooth [51]. These differences and their indirect effects (e.g., heat capacity, wind field, evapotranspiration, etc.) resulted in a significant difference in the SUHII obtained by the two methods, which was much higher than that obtained by the other methods. Furthermore, circular areas (buffer strips) delineated based on varying buffer distances are deemed an appropriate representation of the reference area (suburban or rural) [52]. The buffer zones are typically situated adjacent to the urban boundary, and their dimensions and position can be modified according to the requirements of the study, thus creating a flexible reference area. However, there are no standards for the buffer distances that appear in the existing studies, and few studies have investigated the effect of buffer radius on SUHII. In addition, the diversity

and variability of land cover and land use types within buffer zones introduce more uncertainty in temperature measurements [53]. The findings of this study validate the differences that different buffer distances can bring to SUHII assessment. The mean values of SUHII obtained based on M5 (turning point method) were high, especially in spring, and the difference with other similar methods was very significant. This phenomenon can be attributed to the buffer approach of the method. The buffer was defined as the lowest point in the temperature curve of several continuous buffers. This temperature was typically lower than the reference temperature of other methods, which enabled the attainment of higher SUHII values [54]. Furthermore, there were minor discrepancies between SUHII values obtained by comparable methods, except for M5. This can be attributed to the fact that LST typically declines exponentially with increasing distance from the urban boundary. Despite the disparity in buffer radius among methods, it did not significantly alter the mean LST of the buffer, which consequently resulted in no notable discrepancy in SUHII [40]. It is noteworthy that M8 generated a lower SUHII in the method comparison. Such a result may be caused by the additional thermal impact of neighboring urban patches, particularly in areas with a dense distribution of urban patches.

The dynamic changes in the reference area, represented by seasonal differences, performed as a key factor exacerbating the uncertainty in depicting the spatiotemporal variation patterns of SUHII. On the one hand, SUHII values obtained by the same reference method showed significant seasonal differences (see Fig. 5). On the other hand, SUHII differences estimated based on the same reference methods were not consistent across seasons (see Fig. 6). Although the spatial extent of the reference area is relatively fixed, which helps to control disturbances caused by urbanization, there are interseasonal variations in nonurbanized elements, such as meteorology, biology, soil, and human activities, which drive the reference area to exhibit temporal instability [55]. This will increase the uncertainty in SUHII assessment, leading to inaccurate or even erroneous understanding of the spatial pattern, temporal evolution, and driving mechanisms of the urban surface thermal environment. This consequently poses a challenge to the implementation of multifaceted adaptation-mitigation measures, such as the subsequent policy designation, planning implementation, and individual coping. To quantify SUHII in an objective and universal manner, and to obtain reliable information and knowledge about the characteristics and drivers of the urban surface thermal environment, it is necessary to employ appropriate standardized reference methods, as well as to synthesize the temporal evolution and control potential disturbing factors in nonurban areas.

A series of methods based on image elements or small-scale relative mean patches have been developed to get rid of the uncertainty associated with the urban–rural dichotomy-based SUHII assessment. Among them, LCZs provide a classification criterion for interurban SUHII investigation [56], [57]. In comparison with SUHII calculations based on the urban–rural dichotomy, this approach gives more comprehensive consideration to land cover and building structure characteristics, thereby enhancing the scientific validity and reliability of the results. Concurrently, the meticulous categorization and high spatial resolution characteristics of this approach facilitate the identification of smaller scale microclimate features that are not discernible through the use of an urban-scale methodology. This enables a more detailed and targeted response [58], [59]. However, the LCZ-based SUHII calculation method is still similar to the urban-scale method, which is a simple difference operation between the target LCZ (built LCZ) and the reference LCZ (land cover LCZ), which leads to similar uncertainties in the SUHII estimate. First, previous studies lacked a uniform definition of reference LCZs, which resulted in a lack of comparability and generalizability of the findings. It was demonstrated that the local SUHII obtained based on the MG method was considerably higher than that of other methods. This was attributed to the distinctive physical properties of the water body, which exerted a significant influence on LST. On the one hand, the heat capacity of water bodies is considerably higher than that of soil or vegetation, which can absorb and store more heat. On the other hand, water bodies consume a considerable amount of heat due to the evaporative cooling effect, which leads to a significant reduction in temperature. A lower reference LST leads to an overestimation of the SUHII when the LST of the target LCZ is constant [60], [61]. Similarly, the SUHII was underestimated in the reference case with bare ground with opposite physical properties (low heat capacity and high albedo). It is worth noting that this situation was not robust between seasons, showing poor seasonal consistency (see Fig. 8), which can be attributed to seasonal differences in the mechanisms of land cover action. This was more pronounced on bare ground (LCZ F) where solar radiation was strong in summer and the cover itself heated up faster due to its low heat capacity and high thermal conductivity, resulting in higher daytime LSTs, while in winter, there was less solar radiation and the cover itself had a low heat capacity and lack sufficient insulation to prevent rapid heat loss, resulting in lower daytime temperatures in winter [62]. There were also LST variations in vegetated areas due to different mechanisms. In summer, the transpiration and shading insulation effects of vegetation bring about lower LSTs compared with the surrounding area, while in winter, LSTs are higher compared with the bare surface due to the insulating effect of the canopy and the reduction of ventilation heat from increased surface roughness [63], [64], [65]. Consequently, neglecting perturbations due to differences in the seasonal driving mechanisms of the LCZs themselves and their temperature response, especially the land cover-type LCZs used as references, can introduce uncertainty in local SUHII assessment.

B. Selection Strategy of Reference Methods for SUHII Quantization

To control the uncertainties in SUHII estimate and the associated spatiotemporal pattern exploration, it is imperative to raise effective strategies for optimized reference selections.

Combining the experience of previous studies with the results of this study, the urban-scale reference methods were ranked in order of applicability and reliability as follows: Administrative division method < fixed-distance buffer method < turning point

method < stable landscape method < footprint-based method. First, the least recommended is the division based on administrative regions. This method is only suitable for use in specific cases, where there is a high degree of homogeneity within the region, including topography, meteorology, landscape, and so on [33]. Moreover, nowadays, with the development of urban agglomerations, urban areas show spatial proximity, connectivity, and integration, which strengthens the inapplicability of this type of method [66]. Second, methods for establishing buffer zones immediately adjacent to urban boundaries, such as the M3, M4, M6, and M7 methods. It must be recognized that the temperature of the region beyond the urban boundary can be influenced by the urban area. The difference between the environment inside and outside the boundary increases the advection effect between the regions, leading to a spillover of high temperatures and bringing additional heat to the environment outside the domain [67]. As a result, the urban–rural temperature curve showed a single exponential decline rather than a cliff-like decline as one moved away from the urban boundary. In some studies, the urban–rural gradient has also been defined as the urban, expansion area, and rural levels for analysis of the thermal environment [68]. Therefore, the construction of a buffer zone immediately adjacent to the boundary as a reference area unaffected by urban influence is inappropriate and tends to underestimate SUHII, as verified in this study (see Fig. 5). Likewise, the outer boundary of the buffer zone should not be too far away. Differences in meteorological conditions, landscape and topographic conditions, etc., brought about by excessive distances can also cause disturbances in the estimation of SUHII [69]. In addition to the aforementioned issues, the invariant buffer radius of patches (M3 and M4) and the spatial overlay issues that arise in dense urban areas can give rise to significant uncertainty in the assessment of SUHII [70]. Third, the method using turning point (M5) identified the reference area based on the urban–rural LST gradient and can mitigate the additional impact of urban heat spillover effects. Thus, this method was demonstrated to be superior to the first method. However, this method is also confronted by a series of problems in practical application. It is highly sensitive to outliers and, thus, requires detailed exclusion of potentially influential pixels, especially in large water bodies. The influence of outliers on a regional scale may result in turning points that are not easily identified and increase the cost of computational time. Next, the existing studies were inconsistent in their methods of identifying turning points (visual inspection, locally weighted regression, nonlinear fitting, etc.) [54], [71], [72]. The identification of turning points based on different methods produced disparate results, making it challenging to compare SUHIIs identified through such methods. The fourth is the stable landscape method. This study selected the large water body in the region, Taihu Lake area. In comparison with other methods, large water bodies serve as a reference point with a distinct advantage in estimating SUHII due to their larger volume, spatial and property stability, and less influence of urbanization on temperature. This allows for the effective carrying out of interseasonal and interannual comparisons. The method also exhibits certain limitations. On the one hand, the lower reference temperature of large water bodies results in an overestimation of the absolute value of SUHII. On the other hand, the method is less generalizable, and such a large and stable landscape cannot be found in all regions, which represents the most significant limitation of the method. Finally, the most recommended for the study is the footprint-based method (MF). Although the SUHII obtained based on this method was not significantly different from buffer-based methods, it was designed to take into account the high-temperature spillover effects due to temperature differences between peri-urban environments. Furthermore, despite the differences in specific modeling approaches to quantify the footprint of existing methods, such as Gaussian surface fitting and nonlinear decay models, the underlying premise of these methods is consistent. This is the monotonic decay trend of the urban–rural temperature gradient in the presence of a significant UHI effect [73]. This lays the foundation for enhancing the comparability of the results. It is important to note that, when applying the method, it is essential to maintain independence in the selection of the reference area and to avoid the influence of other urban areas in the vicinity.

On the local scale, the study revealed significant differences in SUHII assessment using different land cover-type LCZs as references (see Fig. 7) and further reported strong inconsistencies in all seasons except summer in spatial patterns (see Fig. 8). Overall, our recommended order of reference zone selection is LCZ C (LCZ D) and LCZ B > LCZ G and LCZA > LCZ F. First, LCZ F, which is the LCZ with the highest similarity to the built-type LCZ, is the least recommended. Due to its high surface albedo and the lack of moderating effect of vegetation cover, there are significant diurnal, seasonal, and interannual variations in its LST, which makes it challenging to achieve a precise SUHII estimate. Next, there are LCZ A and LCZ G, both of which are better than LCZ F in terms of the stability of their internal temperatures. However, their application is limited by their small and scattered distribution, especially in LCZ A, which mostly exists in topographically complex zones and produces complex impacts that are difficult to control. Previous studies have confirmed that blue–green infrastructure reaches a certain size threshold before it can fully exert its cooling effect [74]. Similarly, the internal temperature of smaller and fragmented blue–green patches is highly susceptible to the influence of the surrounding built environment, which, in turn, affects the accuracy of their reference temperature. In contrast, LCZ C (LCZ D) and LCZ B are more widely distributed, with their primary function in urban areas being urban parks. This confers upon them an advantage in terms of being used as a reference for SUHII calculation.

C. Mitigation Strategies, Limitations, and Prospects

In addition to investigating the uncertainties introduced by differences in reference methods, the study also validates the substantial multiscale SUHI effects within this region. In order to offset the detrimental effects of this phenomenon on ecological security and sustainable development, it is imperative to implement a multifaceted approach that integrates policy, planning, and technology in a unified manner. At the macrocity scale, measures should be oriented toward comprehensive planning

and policy development. It is incumbent upon governing bodies to implement rigorous standards of building energy efficiency and to provide appropriate economic incentives with a view to promoting the development, dissemination, and application of cooling technologies and materials. Concurrently, the advancement of blue–green infrastructure and ecological restoration initiatives should be facilitated through the implementation of greening regulations and planning guidelines, with the objective of optimizing urban form and land use [13]. In addition, a real-time monitoring system should be synchronized to provide scientific guidance for policy implementation and adjustment. Furthermore, it is imperative to reinforce regional coordination and collaboration, particularly within urban agglomeration regions, in order to establish comprehensive regional ecological protection and climate regulation systems [75]. This will facilitate the sharing of data, technology, and experience, enabling a collective response to the seasonal UHI effect, which is a consequence of climate change. At the local neighborhood level, mitigation measures should focus on area-specific microclimate improvements, particularly in the compact low-rise (LCZ 3), open low-density (LCZ 8), and compact midrise (LCZ 2) blocks. Adaptations to specific neighborhood characteristics and climatic conditions can be made to achieve more effective UHI mitigation. For example, in high-density areas, such as LCZ 3 and LCZ 2, measures, such as the use of efficient shading devices, green roofs, and improved building design, should be considered to reduce the heat island effect. For low- and medium-density zones, such as LCZ 8, localized warming can be mitigated by measures, such as increasing green roofs, street greening, and the use of cooling materials [76]. In addition, energy-saving retrofitting of buildings should be promoted, such as the installation of high-efficiency air conditioning systems to reduce local heat emissions. These measures can significantly reduce the SUHI effect at the local scale and improve the living comfort of residents.

This study is subject to certain limitations. First, this study explored the seasonal change of the sensitivity of SUHII estimate to the diverse methods of reference delineation, yet the variations on other timescales, e.g., interannual scale or long-term trends, were note considered. Second, the results generated by the remotely sensed LST data may not necessarily apply to those using air temperate data. Future research is encouraged to explore the similarities, differences, and advantages of different reference delineation methods in air temperature-based UHII analysis. Third, the spatial scope of this study is limited to the circum-Taihu Lake cities, which are relatively homogeneous in terms of internal geographic conditions, climatic resources, locational characteristics, and anthropogenic factors. In the future, it is necessary to explore the differences in SUHII assessment results brought about by different reference methods on a larger spatial scope to verify the robustness and applicability of the results. Moreover, due to computational costs, data requirements, and prior knowledge requirements, the existing studies assessing SUHII based on LCZ mostly focused on the local scale [77]. In future studies, we will incorporate such efforts into urban-scale SUHI assessment using the footprint-based method. With the simultaneous delineation of LCZ-based urban and reference areas, the later will be further "refined" and "dynamically controlled" to more stable and homogeneous land cover-type LCZs, thereby enhancing the effectiveness and generalizability of the reference delineation methodology.

V. Conclusion

This study examined the existing urban-scale and local-scale reference delineation methods for SUHII estimate and the associated spatial and seasonal variations, with the specific case of the circum-Taihu Lake region.

At the city scale, the results revealed significant variability among different methods, especially in winter. Higher values of SUHII for all seasons were obtained based on the stable landscape method, while lower values were generated with the equal radius method (spring, autumn, and winter) and the equal area method (summer). In terms of spatial patterns, the spatial heterogeneity of SUHII obtained by reference identified as a specific area was stronger than that based on methods using buffer area references. The SUHIIs obtained by the eight methods exhibited strong spatial consistency in summer and autumn, while they were weaker in spring and winter, or even showed opposite distribution characteristics.

At the local scale, the overall SUHII of built-type LCZs obtained from different land cover references showed the greatest difference in the spring. Across seasons, the SUHII obtained based on the LCZ G reference was higher, while the SUHII obtained based on the LCZ F and LCZ B was lower. Meanwhile, the acquired SUHII results showed strong spatial consistency during summer. For specific built-type LCZs, it was found that the largest intermethod differences in SUHII assessments for LCZ 1, LCZ 2, LCZ 3, LCZ 5, LCZ 8, and LCZ 10 occurred in spring, LCZ 4 in autumn, and LCZ 6 in summer. The spatial patterns and seasonal instability of SUHII obtained based on the different methods also presented differences among built-type LCZs. High spatial pattern consistency was predominantly found in summer (LCZ 1, LCZ 2, LCZ 3, LCZ 4, and LCZ 5) and autumn (LCZ 6, LCZ 8, and LCZ 10), which was lower in spring and winter.

Finally, based on the experience of previous studies and the results of this study, the uncertainties and selection strategies of SUHII assessment methods based on urban–rural division and local climate zoning were summarized. On the urban scale, the applicability was ranked as administrative division method $<$ fixed-distance buffer method $<$ turning point method $<$ stable landscape method $<$ footprint-based method. On the local scale based on LCZ, the ranking was then as LCZ C (LCZ D) and LCZ B $>$ LCZ G and LCZA $>$ LCZ F. This research provides empirical evidence supporting the appropriate nonurban reference delineation for reliable SUHII estimate, which may facilitate improved understanding of the spatiotemporal patterns, evolving processes, underlying mechanisms, and possible solutions of urban heat under rapid urbanization and global climate change.

APPENDIX

See Figs. 9–11.

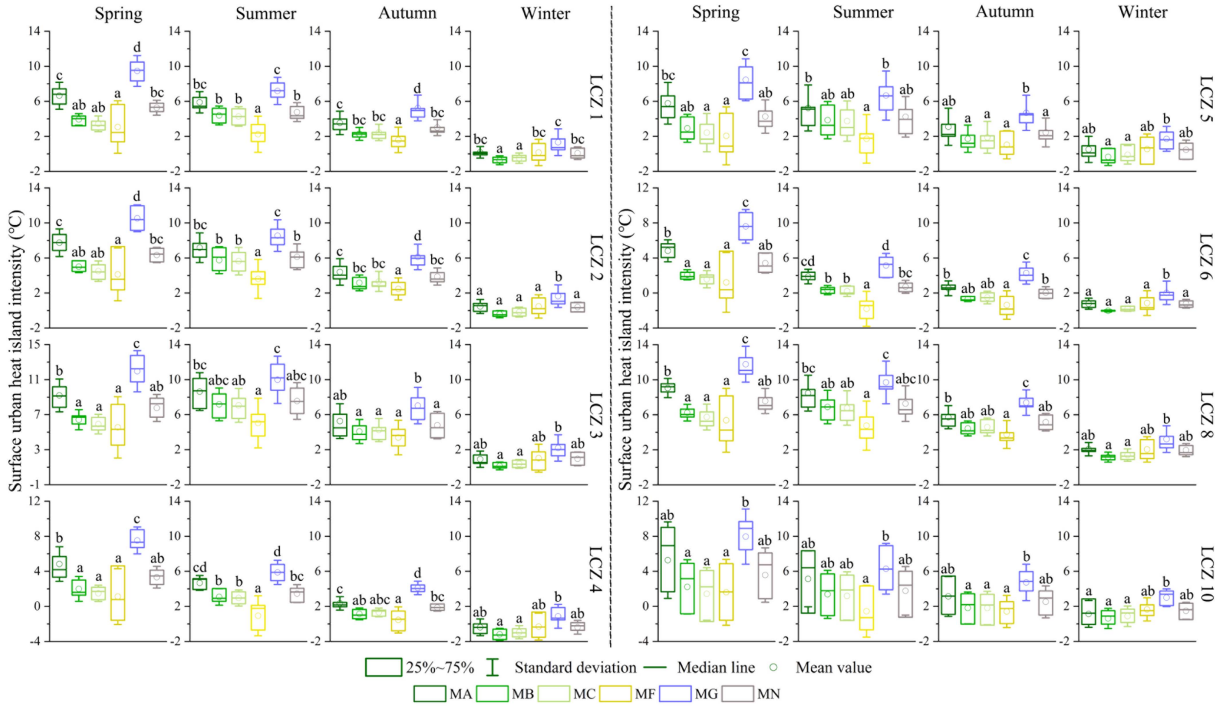

Fig. 9. Local seasonal SUHII of different built-type LCZs based on multiple references defined using different land cover-type LCZs.

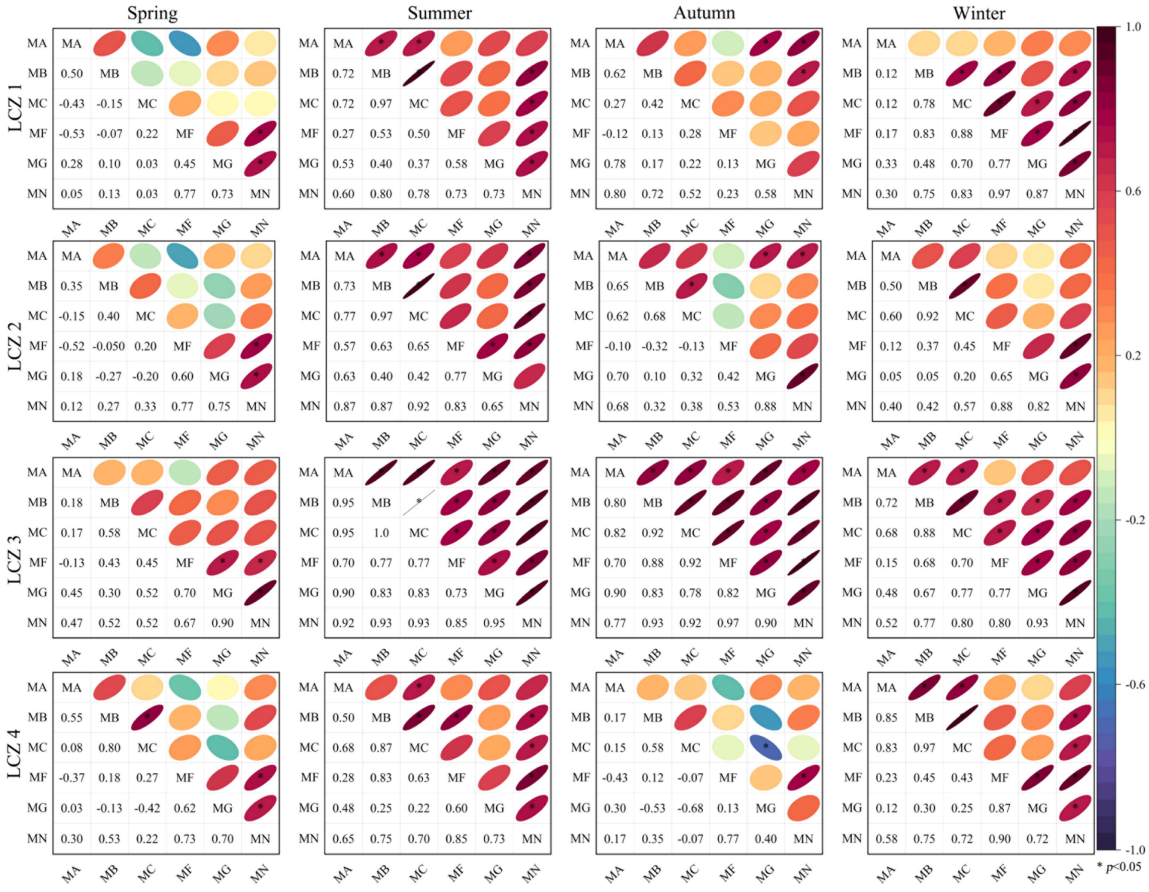

Fig. 10. Correlation coefficients of local-scale SUHIIs of LCZ 1, LCZ 2, LCZ 3, and LCZ 4 between any pair of reference delineation methods for all seasons. Note: Larger ellipse area indicated the greater standard deviation of data distribution.

Fig. 11. Correlation coefficients of the local scale of SUHIIs LCZ 5, LCZ 6, LCZ 8, and LCZ 10 between any pair of reference delineation methods for all seasons. Note: Larger ellipse area indicated the greater standard deviation of data distribution.

REFERENCES

[1] Y. Li, Y. Sun, J. Li, and C. Gao, "Socioeconomic drivers of urban heat island effect: Empirical evidence from major Chinese cities," *Sustain. Cities Soc.*, vol. 63, 2020, Art. no. 102425.

[2] G. Qiu and X. Zhang, "China's urbanization and its ecological environment challenges in the 21st century," *Adv. Earth Sci.*, vol. 34, no. 6, pp. 640–649, 2019.

[3] B.-J. He, "Spatial and socioeconomic heterogeneity of heat-related perception, awareness, knowledge and impacts for unbiased heat action plans," *J. Cleaner Prod.*, vol. 469, 2024, Art. no. 143164.

[4] B.-J. He, W. Wang, A. Sharifi, and X. Liu, "Progress, knowledge gap and future directions of urban heat mitigation and adaptation research through a bibliometric review of history and evolution," *Energy Buildings*, vol. 287, 2023, Art. no. 112976.

[5] J. Zhou, Y. Chen, J. Wang, and W. Zhan, "Maximum nighttime urban heat island (UHI) intensity simulation by integrating remotely sensed data and meteorological observations," *IEEE J. Sel. Topics Appl. Earth Observ. Remote Sens.*, vol. 4, no. 1, pp. 138–146, Mar. 2011.

[6] K. Xiong and B.-J. He, "Planning for heat-resilient educational precincts: Framework formulation, cooling infrastructure selection and walkable routes determination," *Sustain. Cities Soc.*, vol. 101, 2024, Art. no. 105183.

[7] Y. Cui, M. Yin, X. Cheng, J. Tang, and B.-J. He, "Towards cool cities and communities: Preparing for an increasingly hot future by the development of heat-resilient infrastructure and urban heat management plan," *Environ. Technol. Innov.*, vol. 34, 2024, Art. no. 103568.

[8] Q. Wang, X. Wang, Y. Zhou, D. Liu, and H. Wang, "The dominant factors and influence of urban characteristics on land surface temperature using random forest algorithm," *Sustain. Cities Soc.*, vol. 79, 2022, Art. no. 103722.

[9] M. Masoudi and P. Y. Tan, "Multi-year comparison of the effects of spatial pattern of urban green spaces on urban land surface temperature," *Landscape Urban Plann.*, vol. 184, pp. 44–58, 2019.

[10] X. Fu, L. Yao, W. Xu, Y. Wang, and S. Sun, "Exploring the multi-temporal surface urban heat island effect and its driving relation in the Beijing-Tianjin-Hebei urban agglomeration," *Appl. Geogr.*, vol. 144, 2022, Art. no. 102714.

[11] Q. Yang et al., "An adaptive synchronous extraction (ASE) method for estimating intensity and footprint of surface urban heat islands: A case study of 254 North American cities," *Remote Sens. Environ.*, vol. 297, 2023, Art. no. 113777.

[12] T. Ren, W. Zhou, and J. Wang, "Beyond intensity of urban heat island effect: A continental scale analysis on land surface temperature in major Chinese cities," *Sci. Total Environ.*, vol. 791, 2021, Art. no. 148334.

[13] Z. Chen and Y. Zhang, "Quantitative identification of temporal-spatial variations of urban heat island (UHI) effects in Changchun, China," *IEEE J. Sel. Topics Appl. Earth Observ. Remote Sens.*, vol. 15, pp. 3052–3060, Apr. 2022.

[14] Y. Chen, J. Yang, R. Yang, X. Xiao, and J. Xia, "Contribution of urban functional zones to the spatial distribution of urban thermal environment," *Building Environ.*, vol. 216, 2022, Art. no. 109000.

[15] G. Nie et al., "Duration of exposure to compound daytime-nighttime high temperatures and changes in population exposure in China under global warming," *Humanit Soc. Sci. Commun.*, vol. 11, no. 1, 2024, Art. no. 1065.

[16] A. Lin, H. Wu, W. Luo, K. Fan, and H. Liu, "How does urban heat island differ across urban functional zones? Insights from 2D/3D urban morphology using geospatial big data," *Urban Climate*, vol. 53, 2024, Art. no. 101787.

[17] Y. Bai, L. Liu, J. Yang, J. Wang, and Q. Zou, "Drivers of land surface temperatures from the perspective of urban functional zones," *IEEE J. Sel. Topics Appl. Earth Observ. Remote Sens.*, vol. 17, pp. 12274–12285, Jun. 2024.

[18] Q. Zhang et al., "Influence of 2D/3D urban morphology on diurnal land surface temperature from the perspective of functional zones," *IEEE J. Sel. Topics Appl. Earth Observ. Remote Sens.*, vol. 17, pp. 17036–17051, Sep. 2024, doi: 10.1109/JSTARS.2024.3455791.

[19] W. Yu, J. Yang, N. Cong, J. Ren, H. Yu, and X. Xiao, "Attribution of urban diurnal thermal environmental change: Importance of global–local effects," *IEEE J. Sel. Topics Appl. Earth Observ. Remote Sens.*, vol. 16, pp. 8087–8101, Aug. 2023.

[20] J. Mendez-Astudillo and M. Mendez-Astudillo, "A machine learning approach to monitoring the UHI from GNSS data," *IEEE Trans. Geosci. Remote Sens.*, vol. 60, 2022, Art. no. 5800911.

[21] J. Zhao, F. Guo, H. Zhang, and J. Dong, "Mechanisms of non-stationary influence of urban form on the diurnal thermal environment based on machine learning and MGWR analysis," *Sustain. Cities Soc.*, vol. 101, 2024, Art. no. 105194.

[22] W. Yu et al., "How urban heat island magnifies hot day exposure: Global unevenness derived from differences in built landscape," *Sci. Total Environ.*, vol. 945, 2022, Art. no. 174043.

[23] A. Siddiqui, G. Kushwaha, B. Nikam, S. K. Srivastav, A. Shelar, and P. Kumar, "Analysing the day/night seasonal and annual changes and trends in land surface temperature and surface urban heat island intensity (SUHII) for Indian cities," *Sustain. Cities Soc.*, vol. 75, 2021, Art. no. 103374.

[24] R. Yao, X. Huang, Y. Zhang, L. Wang, J. Li, and Q. Yang, "Estimation of the surface urban heat island intensity across 1031 global cities using the regression-modification-estimation (RME) method," *J. Cleaner Prod.*, vol. 434, 2024, Art. no. 140231.

[25] K. Li, D. Lyu, Y. Chen, and J. Jiang, "Classifying seasonal patterns of clear-sky surface urban heat island worldwide and investigating impacts from surface energy variations," *Sustain. Cities Soc.*, vol. 106, 2024, Art. no. 105367.

[26] B. Zheng, Y. Chen, and Y. Hu, "Analysis of land cover and SUHII pattern using local climate zone framework—A case study of Chang-Zhu-Tan main urban area," *Urban Climate*, vol. 43, 2022, Art. no. 101153.

[27] L. Zhang, M. Nikolopoulou, S. Guo, and D. Song, "Impact of LCZs spatial pattern on urban heat island: A case study in Wuhan, China," *Building Environ.*, vol. 226, 2022, Art. no. 109785.

[28] B. Yuan, L. Zhou, F. Hu, and Q. Zhang, "Diurnal dynamics of heat exposure in Xi'an: A perspective from local climate zone," *Building Environ.*, vol. 222, 2022, Art. no. 109400.

[29] Z. Lin, H. Xu, X. Yao, C. Yang, and L. Yang, "Exploring the relationship between thermal environmental factors and land surface temperature of a 'furnace city' based on local climate zones," *Building Environ.*, vol. 243, 2023, Art. no. 110732.

[30] C. Zhao et al., "Long-term trends in surface thermal environment and its potential drivers along the urban development gradients in rapidly urbanizing regions of China," *Sustain. Cities Soc.*, vol. 105, 2024, Art. no. 105324.

[31] J. Gao, J. Gong, J. Yang, J. Li, and S. Li, "Measuring spatial connectivity between patches of the heat source and sink (SCSS): A new index to quantify the heterogeneity impacts of landscape patterns on land surface temperature," *Landscape Urban Plann.*, vol. 217, 2022, Art. no. 104260.

[32] Y. Yao, C. Chang, F. Ndayisaba, and S. Wang, "A new approach for surface urban heat island monitoring based on machine learning algorithm and spatiotemporal fusion model," *IEEE Access*, vol. 8, pp. 164268–164281, 2020.

[33] H. Liu, B.-J. He, S. Gao, Q. Zhan, and C. Yang, "Influence of non-urban reference delineation on trend estimate of surface urban heat island intensity: A comparison of seven methods," *Remote Sens. Environ.*, vol. 296, 2023, Art. no. 113735.

[34] B. Bechtel et al., "SUHI analysis using local climate zones—A comparison of 50 cities," *Urban Climate*, vol. 28, 2019, Art. no. 100451.

[35] Y. Chang, J. Xiao, X. Li, and Q. Weng, "Monitoring diurnal dynamics of surface urban heat island for urban agglomerations using ECOSTRESS land surface temperature observations," *Sustain. Cities Soc.*, vol. 98, 2023, Art. no. 104833.

[36] G. Xian et al., "The effects of urban land cover dynamics on urban heat island intensity and temporal trends," *GISci. Remote Sens.*, vol. 58, no. 4, pp. 501–515, 2021.

[37] Z. Zhang et al., "A mechanistic assessment of urban heat island intensities and drivers across climates," *Urban Climate*, vol. 44, 2022, Art. no. 101215.

[38] J. Liao, Y. Dai, L. An, J. Hang, Y. Shi, and L. Zeng, "Water-energy-vegetation nexus explain global geographical variation in surface urban heat island intensity," *Sci. Total Environ.*, vol. 895, 2023, Art. no. 165158.

[39] X. Yao et al., "How can urban parks be planned to mitigate urban heat island effect in 'furnace cities'? An accumulation perspective," *J. Cleaner Prod.*, vol. 330, 2022, Art. no. 129852.

[40] W. Liao, Z. Cai, Y. Feng, D. Gan, and X. Li, "A simple and easy method to quantify the cool island intensity of urban greenspace," *Urban Forestry Urban Greening*, vol. 62, 2021, Art. no. 127173.

[41] X. Li and W. Zhou, "Optimizing urban greenspace spatial pattern to mitigate urban heat island effects: Extending understanding from local to the city scale," *Urban Forestry Urban Greening*, vol. 41, pp. 255–263, 2019.

[42] Y. Xiao, Y. Piao, C. Pan, D. Lee, and B. Zhao, "Using buffer analysis to determine urban park cooling intensity: Five estimation methods for Nanjing, China," *Sci. Total Environ.*, vol. 868, 2023, Art. no. 161463.

[43] H. Liu, B. Huang, Q. Zhan, S. Gao, R. Li, and Z. Fan, "The influence of urban form on surface urban heat island and its planning implications: Evidence from 1288 urban clusters in China," *Sustain. Cities Soc.*, vol. 71, 2021, Art. no. 102987.

[44] H. Yu and D. Sun, "Quantification of urban heat island effect and differences in regional influence based on footprint analysis: A case study of the Beijing–Tianjin–Hebei urban agglomeration," *IEEE J. Sel. Topics Appl. Earth Observ. Remote Sens.*, vol. 17, pp. 6910–6919, Mar. 2024.

[45] X. Liu, N. Wang, Z. Li, R. Jia, and Z. Qiao, "Research on time series and spatial gradient of urban heat island expansion from the perspective of urban renewal," *IEEE J. Sel. Topics Appl. Earth Observ. Remote Sens.*, vol. 16, pp. 8680–8688, Sep. 2023.

[46] Y. Zhang and J. Cheng, "Spatio-temporal analysis of urban heat island using multisource remote sensing data: A case study in Hangzhou, China," *IEEE J. Sel. Topics Appl. Earth Observ. Remote Sens.*, vol. 12, no. 9, pp. 3317–3326, Sep. 2019.

[47] J. Ching et al., "WUDAPT: An urban weather, climate, and environmental modeling infrastructure for the Anthropocene," *Bull. Amer. Meteorol. Soc.*, vol. 99, no. 9, pp. 1907–1924, 2018.

[48] G. Mills et al., "An introduction to the WUDAPT project," in *Proc. 9th Int. Conf. Urban Climate*, Toulouse, France, 2015, pp. 20–24.

[49] D. Zhou, S. Sun, Y. Li, L. Zhang, and L. Huang, "A multi-perspective study of atmospheric urban heat island effect in China based on national meteorological observations: Facts and uncertainties," *Sci. Total Environ.*, vol. 854, 2023, Art. no. 158638.

[50] L. Tian, J. Yang, and C. Jin, "Dynamic changes in land cover and its effect on urban heat islands," *IEEE J. Sel. Topics Appl. Earth Observ. Remote Sens.*, vol. 17, pp. 2386–2395, 2024.

[51] S. Varamesh, S. M. Anbaran, B. Shirmohammadi, N. Al-Ansari, S. Shabani, and A. Jaafari, "How do different land uses/covers contribute to land surface temperature and albedo?," *Sustainability*, vol. 14, no. 24, 2022, Art. no. 16963.

[52] Y. Chang, J. Xiao, X. Li, D. Zhou, and Y. Wu, "Combining GOES-R and ECOSTRESS land surface temperature data to investigate diurnal variations of surface urban heat island," *Sci. Total Environ.*, vol. 823, 2022, Art. no. 153652.

[53] J. Sun and S. Ongsomwang, "Impact of multitemporal land use and land cover change on land surface temperature due to urbanization in Hefei City, China," *ISPRS Int. J. Geo-Inf.*, vol. 10, no. 12, 2021, Art. no. 809.

[54] K. Qiu and B. Jia, "The roles of landscape both inside the park and the surroundings in park cooling effect," *Sustain. Cities Soc.*, vol. 52, 2020, Art. no. 101864.

[55] D. Sun, C. Hu, Y. Wang, Z. Wang, and J. Zhang, "Examining spatio-temporal characteristics of urban heat islands and factors driving them in Hangzhou, China," *IEEE J. Sel. Topics Appl. Earth Observ. Remote Sens.*, vol. 14, pp. 8316–8325, Aug. 2021.

[56] G. Chen, Y. Chen, X. Tan, L. Zhao, Y. Cai, and L. Li, "Assessing the urban heat island effect of different local climate zones in Guangzhou, China," *Building Environ.*, vol. 244, 2023, Art. no. 110770.

[57] Y. Xi, S. Wang, Y. Zou, X. Zhou, and Y. Zhang, "Seasonal surface urban heat island analysis based on local climate zones," *Ecol. Indicators*, vol. 159, 2024, Art. no. 111669.

[58] H. Zhang et al., "Application and future of local climate zone system in urban climate assessment and planning—Bibliometrics and meta-analysis," *Cities*, vol. 150, 2024, Art. no. 104999.
[59] C. Zhao, Q. Weng, Y. Wang, Z. Hu, and C. Wu, "Use of local climate zones to assess the spatiotemporal variations of urban vegetation phenology in Austin, Texas, USA," *GISci. Remote Sens.*, vol. 59, no. 1, pp. 393–409, 2022.
[60] N. Hu, G. Wang, Z. Ma, Z. Ren, M. Zhao, and J. Meng, "The cooling effects of urban waterbodies and their driving forces in China," *Ecol. Indicators*, vol. 156, 2023, Art. no. 111200.
[61] X. Sun, X. Tan, K. Chen, S. Song, X. Zhu, and D. Hou, "Quantifying landscape-metrics impacts on urban green-spaces and water-bodies cooling effect: The study of Nanjing, China," *Urban Forestry Urban Greening*, vol. 55, 2020, Art. no. 126838.
[62] S. Yuan, Z. Ren, X. Shan, Q. Deng, and Z. Zhou, "Seasonal different effects of land cover on urban heat island in Wuhan's metropolitan area," *Urban Climate*, vol. 49, 2023, Art. no. 101547.
[63] E. Massaro et al., "Spatially-optimized urban greening for reduction of population exposure to land surface temperature extremes," *Nature Commun.*, vol. 14, no. 1, 2023, Art. no. 2903.
[64] Z. Guo et al., "Plant canopies exhibit stronger thermoregulation capability at the seasonal than diurnal timescales," *Agricultural Forest Meteorol.*, vol. 339, 2023, Art. no. 109582.
[65] Y. Li et al., "Role of the urban plant environment in the sustainable protection of an ancient city wall," *Building Environ.*, vol. 187, 2021, Art. no. 107405.
[66] J. Li, F. Wang, Y. Fu, B. Guo, Y. Zhao, and H. Yu, "A novel SUHI referenced estimation method for multicenters urban agglomeration using DMSP/OLS nighttime light data," *IEEE J. Sel. Topics Appl. Earth Observ. Remote Sens.*, vol. 13, pp. 1416–1425, Apr. 2020.
[67] Z. Liu et al., "Urban heat islands significantly reduced by COVID-19 lockdown," *Geophysical Res. Lett.*, vol. 49, no. 2, 2022, Art. no. e2021GL096842.
[68] M. Zargari, A. Mofidi, A. Entezari, and M. Baaghideh, "Climatic comparison of surface urban heat island using satellite remote sensing in Tehran and suburbs," *Sci. Rep.*, vol. 14, no. 1, 2024, Art. no. 643.
[69] T. Chakraborty and X. Lee, "A simplified urban-extent algorithm to characterize surface urban heat islands on a global scale and examine vegetation control on their spatiotemporal variability," *Int. J. Appl. Earth Observ. Geoinf.*, vol. 74, pp. 269–280, 2019.
[70] J.-H. Park and G.-H. Cho, "Examining the association between physical characteristics of green space and land surface temperature: A case study of Ulsan, Korea," *Sustainability*, vol. 8, no. 8, 2016, Art. no. 777.
[71] H. Du, W. Cai, Y. Xu, Z. Wang, Y. Wang, and Y. Cai, "Quantifying the cool island effects of urban green spaces using remote sensing data," *Urban Forestry Urban Greening*, vol. 27, pp. 24–31, 2017.
[72] X. Cheng, B. Wei, G. Chen, J. Li, and C. Song, "Influence of park size and its surrounding urban landscape patterns on the park cooling effect," *J. Urban Plann. Develop.*, vol. 141, no. 3, 2015, Art. no. A4014002.
[73] L. Yao, S. Sun, C. Song, J. Li, W. Xu, and Y. Xu, "Understanding the spatiotemporal pattern of the urban heat island footprint in the context of urbanization, a case study in Beijing, China," *Appl. Geogr.*, vol. 133, 2021, Art. no. 102496.
[74] R. C. Estoque, Y. Murayama, and S. W. Myint, "Effects of landscape composition and pattern on land surface temperature: An urban heat island study in the megacities of Southeast Asia," *Sci. Total Environ.*, vol. 577, pp. 349–359, 2017.
[75] J. Ren, J. Yang, W. Yu, N. Cong, X. Xiao, and J. Xia, "Mapping of local climate zones and heat hazard assessment from a historical-future perspective," *IEEE J. Sel. Topics Appl. Earth Observ. Remote Sens.*, vol. 17, pp. 12622–12636, Jul. 2024.
[76] W. Wang and B.-J. He, "Assessment of vertical cooling performance of trees over different surface covers," *J. Thermal Biol.*, vol. 119, 2024, Art. no. 103779.
[77] J. Han, N. Mo, J. Cai, L. Ouyang, and Z. Liu, "Advancing the local climate zones framework: A critical review of methodological progress, persisting challenges, and future research prospects," *Humanities Social Sci. Commun.*, vol. 11, no. 1, 2024, Art. no. 538.

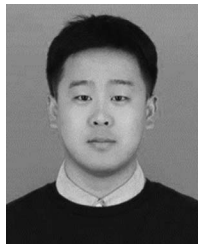

Xuecheng Fu was born in Qingdao, China, in 1997. He received the B.Sc. degree specializing in geographic information science and the M.Sc. degree specializing in cartography and geographic information system from Shandong Normal University, Jinan, China, in 2020 and 2023, respectively. He is currently working toward the Ph.D. degree in architecture with Chongqing University, Chongqing, China, under the supervision of Prof. Bao-Jie He.

His current research interest is in the fields of urban ecology and sustainable built environments. He is a student member of the Geographical Society of China and the Ecological Society of China.

Bao-Jie He received the Ph.D. degree in philosophy from the University of New South Wales, Sydney, NSW, Australia.

He is currently a Full Professor of urban climate and sustainable built environment with the School of Architecture and Urban Planning, Chongqing University, Chongqing, China. He is also a Leader with the Centre for Climate-Resilient and Low-Carbon Cities, Chongqing University, Chongqing, China, Adjunct Associate Professor with the University of Queensland, Brisbane, QLD, Australia, and an Honorary Research Fellow of Hiroshima University, Hiroshima, Japan.

Huimin Liu received the Ph.D. degree in urban and rural planning from Wuhan University, Wuhan, China, in 2019.

She was a Postdoctoral Fellow with the Institute of Space and Earth Information Science, The Chinese University of Hong Kong, Hong Kong. She is currently an Associate Professor with the School of Urban Design, Wuhan University, Wuhan. In 2023, she was selected for the Hubei Province High-Level Talent Program. She is also the Deputy Director with Digital and Smart City Research Institute, Digital City Research Center, Wuhan University, Wuhan. She has authored or coauthored about 30 papers in prominent peer-reviewed journals. Her research interests include the intersection of geography, remote sensing, and urban planning, with a particular focus on the causes, effects, and solutions to urban climate change. She has been invited to review the work report of the U.N. Economic and Social Commission for Asia and the Pacific.